Development 129, 1261-1272 (2002)
Printed in Great Britain © The Company of Biologists Limited 2002
DEV0385

Identification of a developmental transition in plasmodesmatal function during embryogenesis in *Arabidopsis thaliana*

Insoon Kim, Frederick D. Hempel†, Kyle Sha, Jennifer Pfluger and Patricia C. Zambryski*

Department of Plant and Microbial Biology, 111 Koshland Hall, University of California, Berkeley, CA 94720, USA
†Present address: Mendel Biotechnology, 21375 Chabat Blvd, Haywood, CA 94545, USA
*Author for correspondence (e-mail: zambrysk@nature.berkeley.edu)

Accepted 8 November 2001

SUMMARY

Plasmodesmata provide routes for communication and nutrient transfer between plant cells by interconnecting the cytoplasm of adjacent cells. A simple fluorescent tracer loading assay was developed to monitor patterns of cell-to-cell transport via plasmodesmata specifically during embryogenesis. A developmental transition in plasmodesmatal size exclusion limit was found to occur at the torpedo stage of embryogenesis in *Arabidopsis*; at this time, plasmodesmata are down-regulated, allowing transport of small (approx. 0.5 kDa) but not large (approx. 10 kDa) tracers. This assay system was used to screen for embryo-defective mutants, designated *increased size exclusion limit of plasmodesmata* (*ise*), that maintain dilated plasmodesmata at the torpedo stage. The morphology of *ise1* and *ise2* mutants discussed here resembled that of the wild-type during embryo development, although the rate of their embryogenesis was slower. The *ISE1* gene was mapped to position 13 cM on chromosome I using PCR-based biallelic markers. *ise2* was found to be allelic to the previously characterized mutant *emb25* which maps to position 100 cM on chromosome I. The results presented have implications for intercellular signaling pathways that regulate embryonic development, and furthermore represent the first attempt to screen directly for mutants of *Arabidopsis* with altered size exclusion limit of plasmodesmata.

Key words: *Arabidopsis thaliana*, Plant embryo, Intercellular signaling, *ise*, Plasmodesmata, Size exclusion limit

INTRODUCTION

Plant cells are connected via plasmodesmata, cytoplasmic channels that transverse plant cell-walls. Plasmodesmata provide symplastic continuity between cells, facilitating communication and allowing co-ordination of growth and development. Plasmodesmata are plasma membrane-lined and have a core of modified endoplasmic reticulum (ER) in their center (Robards, 1971; Tilney et al., 1991). Transport through plasmodesmata is thought to occur primarily through the cytoplasmic space between the plasma membrane and modified ER (Ding et al., 1992; Gunning, 1976; Overall et al., 1982). An important measure of plasmodesmatal function is their size exclusion limit (SEL), the upper limit in the size of macromolecules that can freely diffuse from cell to cell (Goodwin, 1983; Kempers et al., 1993; Kempers and Van Bel, 1997; Tucker, 1982). The aperture of plasmodesmata is regulated temporally, spatially, and physiologically throughout the development of a plant, although SEL may be fixed in certain cell types or at specific stages of development (for reviews, see Botha and Cross, 2000; Ding, 1998; Jackson, 2000; Pickard and Beachy, 1999; Zambryski and Crawford, 2000).

Work to date on plasmodesmata has focused primarily on their ultrastructure (Ding et al., 1992), their roles during the spread of plant viruses (Carrington et al., 1996; Lazarowitz and Beachy, 1999), and their SEL and functional state in different tissues or during different stages of postgermination development (Crawford and Zambryski, 2000; Crawford and Zambryski, 2001; Duckett et al., 1994; Gisel et al., 1999; Oparka et al., 1999). Furthermore, recent work implies plasmodesmata have critical roles during complex morphogenesis, selectively allowing movement of some, but not all, transcription factors in the apical meristem (Hantke et al., 1995; Lucas et al., 1995; Sessions et al., 2000). Plasmodesmata are also important players in plant defense, most dramatically illustrated in the recent wealth of data on gene silencing (Baulcombe, 2001; Mourrain et al., 2000; Palauqui and Balzergue, 1999; Palauqui et al., 1997; Voinnet et al., 1998; Voinnet et al., 2000).

Despite the abundance of information on the structure and function of plasmodesmata, there are few reports that aim to identify the genes that control plasmodesmata architecture or regulatory components (Chisholm et al., 2000; Lartey et al., 1998; Russin et al., 1996). Thus, we set out to specifically design a genetic screen to identify mutants with altered plasmodesmata. The screen begins with the premise that plants with defective plasmodesmata would likely have growth abnormalities, and that homozygous mutants might not survive beyond early seedling stages. Therefore, we focused our

genetic screen on *Arabidopsis* mutant lines segregating embryo-defective phenotypes. Such lines are maintained and propagated as heterozygotes, but their siliques bear homozygous mutant embryos.

A protocol to assess plasmodesmatal SEL during embryo development was designed. Embryos were first removed from their seed coats and then incubated in the presence of fluorescent hydrophilic symplastic tracers. Movement of small and large tracers between cells of embryos was subsequently monitored microscopically. Studies with low molecular mass tracers (approx. 0.5 kDa) revealed that the *Arabidopsis* wild-type embryo consisted of a single symplastic domain, wherein all cells are cytoplasmically interconnected via functional plasmodesmata until late in embryo development. Assays using large tracers (approx. 10 kDa) indicated a decrease in plasmodesmatal SEL in wild-type embryos that initiates in the torpedo stage of development. Two mutant lines, *increased size exclusion limit of plasmodesmata* (*ise*), *ise1* and *ise2*, are distinct from wild-type embryos in allowing the symplastic movement of large 10 kDa dextran probes during, and subsequent to, the torpedo stage of embryo development.

MATERIALS AND METHODS

Isolation of embryo-defective mutants with increased SEL

Stages of embryonic development of *Arabidopsis thaliana* were adapted from Meinke (Meinke, 1994) and West and Harada (West and Harada, 1993). M_2 ethyl methane sulfonate (EMS) mutagenized seeds were purchased from Lehle Seeds (#M2E-04-06, ecotype Landsberg *erecta*, Round Rock, TX, USA). 13,000 lines were screened visually for altered embryo morphology at the torpedo stage of development. 5,000 lines segregating embryo-defective phenotypes were assayed for increased SEL. We focused on two mutants that showed a similar, dramatic increase in SEL (*ise1* and *ise2*). Twelve additional mutants with less dramatic tracer movement phenotypes were also identified, but have not been further characterized. We also assayed a number of known mutants, including some from the collection of Meinke and colleagues (Franzmann et al., 1995) (http://mutant.lse.okstate.edu/embryopage/embryopage.html). One known mutant, *emb25* (Franzmann et al., 1989) also showed an increased SEL. It was subsequently found allelic to *ise2* by genetic complementation.

Probe-movement assays on embryos

Siliques were opened using fine forceps and all seeds were collected. Typically, each silique contained an average of 60 seeds. Seeds were placed on a glass microscope slide with 15-20 μl of 1/2 Murashige and Skoog (MS) liquid culture medium containing fluorescent tracer solutions (see below). A cover slip (22×22 mm) was placed over this solution, and embryos were released from their seed coats by slight tapping with a fingertip or a cotton swab. Embryos were incubated in tracer solutions for 5 minutes at room temperature. Fluorescent tracers were then washed out from under the cover slip with excessive 1/2 MS solution. A cotton swab was placed on one side of cover slip to absorb washing medium and 1/2 MS solution was added to the other side of cover slip. This procedure was repeated until no apparent tracer remained in the solution under the cover slip. Embryos were then immediately observed by fluorescent microscopy. We initially examined probe movement in wild-type embryos to establish the foundation for the mutant screen.

Plant growth

Plants were grown at 22°C in a greenhouse. Seeds were sown on the surface of a 1:1 mix of Sunshine-mix (Fisons Horticultural Inc., Bellevue, WA, USA) and vermiculite. Flats with pots were placed at 4°C for 4 days before germination. Plants were initially grown in short-day conditions, 8 hour light/16 hours dark cycle, for 2 weeks, to increase vegetative growth and subsequent inflorescence vigor. Plants were then transferred to long-day conditions, 16 hours light/8 hours dark cycle to induce flowering.

Fluorescent probes

HPTS (8-hydroxypyrene-1,3,6-trisulfonic acid; mol. mass 524 Da, Molecular Probes, H-348, Eugene, OR, USA) was prepared in 1/2 MS liquid culture medium at 5 mg/ml. Fluorescein isothiocyanate (FITC)-conjugated dextrans (Sigma, FD-10S, St. Louis, MO, USA) were prepared in 1/2 MS at 5 mg/ml. 10 kDa F-dextrans were purified using a sizing column with a 10 kDa cut-off (Amicon, YM-10 Microcon filters, Bedford, MA, USA), to remove low molecular mass contaminants present in commercially prepared FTIC-conjugated dextrans (Oparka, 1991). All fluorescent probes were prepared just before the movement assay.

Fluorescent microscopy

Embryos loaded with fluorescent tracers were analyzed using a Zeiss Axiophot epifluorescence microscope equipped with mercury high-intensity light source and a color CCD camera (Optronics, Goleta, CA, USA). Screening for embryos loaded with fluorescent dyes was carried out by direct observation. Images were captured using Scion Image 1.60 for CG7 software (Scion Corp., Frederick, MD, USA). HPTS and FITC-dextran were analyzed using a Zeiss FITC filter set (exciter BP470/20; dichroic beam splitter 510; emitter LP520), and a Chroma FITC filter set (exciter BP480/30; dichroic beam splitter LP505; emitter BP535/40). Embryos were also observed with a Zeiss 510 confocal laser scanning microscope system, equipped with Argon ion (488 nm) for HPTS and FITC fluorescence, and helium neon lasers (543 nm), to monitor chlorophyll autofluorescence and the cytoplasmic localization of fluorescent tracers (Carl Zeiss, Inc., Thornwood, NY, USA). Images were reconstructed using Adobe Photoshop software (Adobe, San Jose, CA, USA).

Light and scanning electron microscopy

For light microscopy, seeds were frozen in a Bal-Tec HPM 010 High Pressure Freezer (Bal-Tec, Liechtenstein) and subsequently freeze substituted in 2% osmium tetroxide, 0.2% uranyl acetate in acetone. Following high pressure freeze substitution, samples were infiltrated with a decreasing series of acetone:LR white resin and embedded in fresh LR White resin (Ted Pella, CA, USA). Individual seeds were mounted on blocks and sectioned to a thickness of 1 μm using a diamond knife. Sections were heat-fixed to microscope slides, stained with 1% Toluidine Blue plus 1% borax for 4-5 seconds, and washed with distilled water. Coverslips were mounted with Merko-Glass and slides were examined using a Zeiss Axiophot microscope with bright-field optics. Dissecting microscope images of isolated embryos and seedlings and Nomarski images of embryos were obtained as described elsewhere (Meinke, 1994).

For scanning electron microscopy, seedling roots were fixed in FAA (3.7% formaldehyde, 50% ethanol, 5% acetic acid) for 24 hours at 4°C and stored in 70% ethanol. Following dehydration through a graded ethanol series at 4°C the tissue was critical point dried in liquid carbon dioxide. Samples were mounted on stubs and coated with 20 nm of palladium and photographed using a DS-130 scanning electron microscope (International Scientific Instruments, Santa Clara, CA, USA) with an accelerating voltage of 10 kV.

Genetic analysis

Segregation analyses and complementation tests were performed as described elsewhere (Koornneef et al., 1998). Homozygous *ise* mutants are sterile. Therefore, heterozygotes were used to propagate the mutation and to perform genetic crosses. Heterozygous plants were identified by

screening five consecutive siliques for the presence of 25% mutant seeds. Reciprocal crosses were performed between the *ise* mutants. F_1 seeds from an average of 10 siliques from each cross were analyzed. Two *ise* mutants were considered allelic if their F_1 seeds segregated wild-type to mutants at a ratio of 3:1 and non-allelic if all F_1 were wild type.

Molecular mapping

To determine the map position of *ISE* genes using molecular markers, heterozygous +/*ise* plants (Landsberg *erecta*; L*er*) were crossed to wild-type female plants of Columbia (Col) ecotype to introduce polymorphism into mutant lines (Glazebrook et al., 1998). In the resulting F_1 generation, 50% of plants were wild-type and 50% were heterozygous for the *ise* mutation. Heterozygous F_1 plants were allowed to self and F_2 segregating populations were used for mapping. F_2 plants segregated for DNA polymorphism between L*er* and Col, as well as the mutant phenotype. The wild type:heterozygote segregation ratio was 1:2, indicating the mutant phenotype was the result of a single nuclear gene mutation. Homozygous F_2 individuals were used for mapping. Mutant homozygotes do not survive on soil, and were not available for DNA extraction. F_2 wild-type plants, containing the reciprocal products of meiotic recombination, were used for DNA analyses. Mapping was achieved using cleaved amplified polymorphic sequences (CAPS) markers (Glazebrook et al., 1998) (http://www.*Arabidopsis*.org/aboutcaps.html), and simple sequence length polymorphisms (SSLP) markers (Schaffner, 1996) (http://genome.bio.upenn.edu/SSLP_info/SSLP.html). Once linkage to a particular DNA marker was detected, the recombination frequency between the DNA marker and the *ISE* locus was determined and converted to map distance (Koornneef and Stam, 1992).

RESULTS

Strategy to identify mutant embryos with increased SEL of plasmodesmata

Alterations of plasmodesmatal function are likely to lead to defects in overall plant development, and might be expected to manifest as morphological defects that first appear during embryo development. Thus, to identify plasmodesmata mutants, we screened mutant embryos of M_2 lines generated by EMS seed mutagenesis. Note, the logic and mechanics of the genetic screen are presented first. However, this screen is based on our observations of fluorescent tracer uptake during wild-type embryogenesis (see below).

The chronological stages of embryo development in *Arabidopsis* are summarized in Fig. 1. The strategy used to identify mutants with *increased size exclusion limits* (*ise*) is illustrated in Fig. 2. Screening for *ise* mutants was conducted in two steps. First, mutants with altered morphology in the torpedo stage of embryo development were identified under bright-field illumination. Second, mutant and wild-type sibling embryos were incubated with fluorescently labeled 10 kDa dextrans that normally do not traffic cell-to-cell in wild-type mid-torpedo embryos (Figs 3, 4). After extensive washing, embryos were observed using epifluorescence illumination to determine if the F-dextran moved freely between the cells of embryos. Initial probe uptake occurred through cells that were broken during removal of embryos from their seed coats (see Figs 3, 4, 5).

Heart and torpedo embryos (Fig. 1) emit red fluorescence upon blue light excitation, due to the presence of chlorophyll in cells. In contrast, a small subset of the morphologically mutant embryos emit green fluorescence following incubation with 10 kDa F-dextran indicating this large tracer has trafficked cell to cell (diagrammed in lower panel of Fig. 2, and shown in Fig. 6F,G). Visual screening of 13,000 lines identified 5000 lines segregating for morphological defects at the torpedo stage of embryogenesis. Fourteen of these 5000 embryo mutant lines allowed traffic of 10 kDa F-dextrans at the mid-torpedo stage of development compared to wild-type (see below). Two mutants, *ise1* and *ise2*, segregated as single recessive loci, and were characterized further. Complementation studies revealed *ise1* and *ise2* are independent loci.

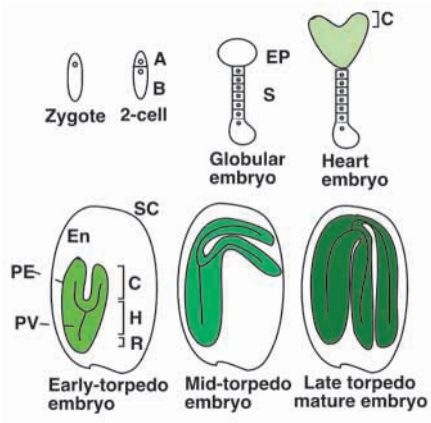

Fig. 1. Schematic representation of stages of embryo development in *Arabidopsis*. The zygote divides to from an embryo composed of a filamentous suspensor (S) that maintains contact with maternal tissues, and a terminal embryo proper (EP). The embryo becomes green at the heart stage of development when chlorophyll and chloroplasts first form. The suspensor degenerates during the torpedo stage. This diagram was adapted from more detailed descriptions of embryo development (Meinke, 1994; West and Harada, 1993) and simplified to highlight stages related to the study reported here. A, apical cell; B, basal cell; C, cotyledon; PE, protoderm; PV, provascular tissues; H, hypocotyl; R, radicle; SC, seed coat; En, endosperm.

Symplastic tracer movement in wild-type embryos

The above strategy was developed specifically to screen embryos relatively late in embryo development, during the early to mid-torpedo stages. This time was chosen for several reasons. First, our screen is challenging as it requires extensive fluorescent microscopy. It is essential that embryos, and their individual cells, are large enough to be viewed easily under low magnification during large scale screening. Torpedo embryos have developed the overall plant body organization, with elongated cotyledons and root initials, and embryos with morphological defects can be distinguished easily at this stage (Goldberg et al., 1994; Mayer et al., 1991). Furthermore, size is important for the critical wash step to remove excess fluorescent probe; earlier staged embryos are much smaller and are often lost during this procedure. Most importantly, we distinguished a developmental change in plasmodesmatal function in wild-type embryos particularly during this time frame; this latter result was uncovered in our characterization of tracer movement in wild-type embryos described below.

Wild-type embryos were screened for their ability to take up small and large fluorescent tracers. HPTS (524 Da) is widely used as a low molecular mass symplastic tracer. HPTS is stable, non-toxic, membrane impermeable, and confined to the cytoplasm and nuclei once it is introduced into cells (Wright and Oparka, 1996). The results in Fig. 3A-D show that HPTS

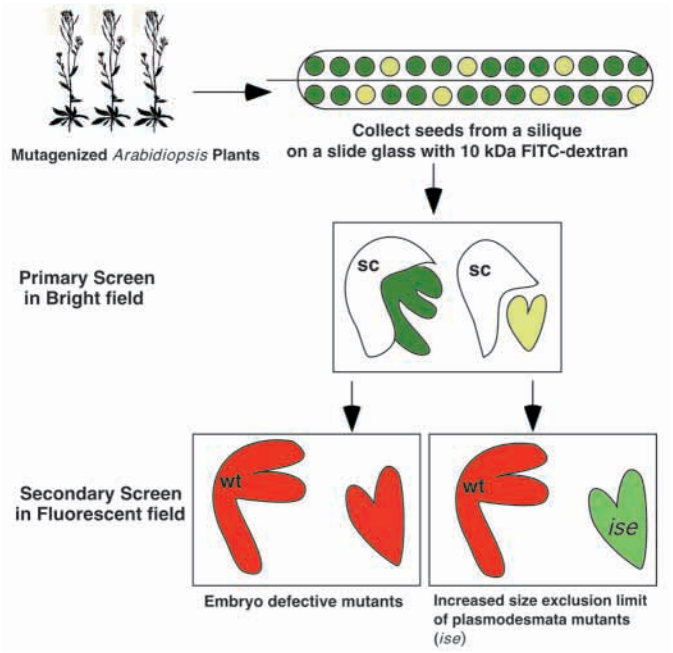

Fig. 2. Genetic screen for *ise* mutants Mature *Arabidopsis* siliques contain about 60 seeds; roughly half are drawn for simplicity. Dark green seeds contain wild-type embryos, and light green seeds contain defective embryos. Embryos were released from their seed coats (sc) and viewed under bright-field illumination. In the example diagrammed here, wild-type is dark green and has reached the mid-torpedo stage, while the mutant is light green and retarded in morphological development (see Fig. 6B,C,D for in vivo results). Embryos were incubated with 10 kDa F-dextran for 5 minutes at room temperature, washed extensively, then viewed by fluorescence microscopy. Wild-type (wt) and most morphologically defective embryos emit red autoflorescence due to cholorophyll, and are unable to transport 10 kDa dextran (left bottom panel). A small fraction of embryo-defective lines (called *increased size exclusion of plasmodesmata*, *ise*) take up and allow movement of 10 kDa F-dextran, and thus exhibit green fluorescence (right bottom panel).

moves freely between all cells of wild-type embryos, indicating that their plasmodesmata allow the passive diffusion of small molecules, and that their SELs are larger than 0.5 kDa. HPTS movement was first observed in globular embryos (not shown). In early heart embryos, cytoplasmic and strong nuclear (Fig. 3A, arrowhead) fluorescence was observed. Apoplastic regions, corresponding to the cell walls, were devoid of HPTS and appeared as dark lines between cells (Fig. 3A, arrow); thus, HPTS evidently does not traffic via the apoplastic pathway in embryos. The same pattern of symplastic movement is evident in late heart (Fig. 3B), early torpedo (Fig. 3C) and mid-torpedo (Fig. 3D) embryos. In mid-torpedo embryos, well-arranged cell files are apparent in both cotyledons and hypocotyls (Fig. 3I). At higher magnification, cytoplasm, nuclei and chloroplasts are clearly distinguished, and the cell wall space between cells is devoid of fluorescence (Fig. 3J-L). Thus, all cells in embryos of all stages of embryogenesis analyzed here contain open and functional plasmodesmata allowing traffic of low molecular mass tracer. These data suggest that the embryo consists of a single symplastic domain, whereas adult plants contain several symplastic domains, for example in young versus more mature tissues (Crawford and Zambryski, 2001; Duckett et al., 1994; Gisel et al., 1999).

F-dextrans, 10 kDa and larger, are used extensively to monitor plasmodesmata SEL in leaf tissues. Microinjection and high pressure biolistic methods for introduction of tracers showed that leaf cells restrict the movement of such large probes (Itaya et al., 2000; Kempers et al., 1993; Oparka and Prior, 1992; Waigmann et al., 1994; Wolf et al., 1989). Recent less invasive methods, such as low pressure biolistic bombardment and loading of tracers through the vascular system has revealed that many leaf cells contain dilated plasmodesmata, allowing traffic of green fluorescent protein (GFP, 27 kDa) and dextrans of at least 20 kDa (Crawford and Zambryski, 2000; Imlau et al., 1999; Oparka et al., 1999). Thus, here we assessed embryos for their ability to traffic large F-dextrans using simple non-pressure loading of tracer through small areas, where cells were broken during removal of embryos from their seed coats.

Movement of 10 kDa F-dextran was assessed in wild-type embryos at different developmental stages. Movement frequencies at each developmental stage were scored and summarized in Table 1. Two surprising results were obtained. First, young embryos, up to the heart stage of development were able to traffic 10 kDa F-dextrans. This result supports recent findings that the SEL of plasmodesmata is high, especially in young tissues (Crawford and Zambryski, 2001). Second, there is a transition between the early and mid-torpedo stages where embryos cease to traffic 10 kDa probes. In a typical wild-type preparation, 50% of heart embryos tested (9 out of 18) were loaded with 10 kDa F-dextrans (Fig. 3E,F). 19.4% of early torpedo embryos were loaded (7 out of 36) (Fig. 3G), but no mid-torpedo embryos were loaded (58 tested) (Fig. 3H). Thus, embryos restrict symplastic movement of 10 kDa F-dextrans as they mature.

The pattern of symplastic movement during wild-type embryogenesis was assessed also using 3 kDa F-dextran. The results obtained were identical to those seen with HPTS, i.e., movement throughout the entire embryo from heart to late torpedo stages (not shown). That 3 kDa dextrans move throughout embryogenesis suggests that plugging of plasmodesmata by callose deposition is unlikely to explain the stage specific down-regulation of 10 kDa F-dextran symplastic movement, as such deposition leads to inhibition of movement of even small tracers such as Lucifer Yellow (Moore-Gordon et al., 1998).

Location and direction of probe uptake

Studies with 10 kDa tracer provide insight into the *location* and *direction* of probe traffic and uptake. Embryos that fail to take up dextrans typically have small patches of fluorescence either at the hypocotyl-cotyledon junction, or at the tip of the radicle (Fig. 3G,H). Probes are evidently taken up initially into a subset of the cells most susceptible to damage during removal of the embryos from their seed coats, for example, in the area of folding of the cotyledons, or the more exposed and protrusive radicle tip, as well as in the fragile region of the suspensor/radicle connection. If the SEL is smaller than the size of the probe, further symplastic movement of probes does not occur. This is illustrated in Fig. 4A, with yellow jagged lines indicating areas most often damaged and black jagged lines indicating areas less frequently damaged. Fig. 4B shows the pattern of 10 kDa F-dextran movement into cells specifically, and only, at the bottom edge of a detached cotyledon from a wild-type mid-torpedo embryo; cytoplasmic

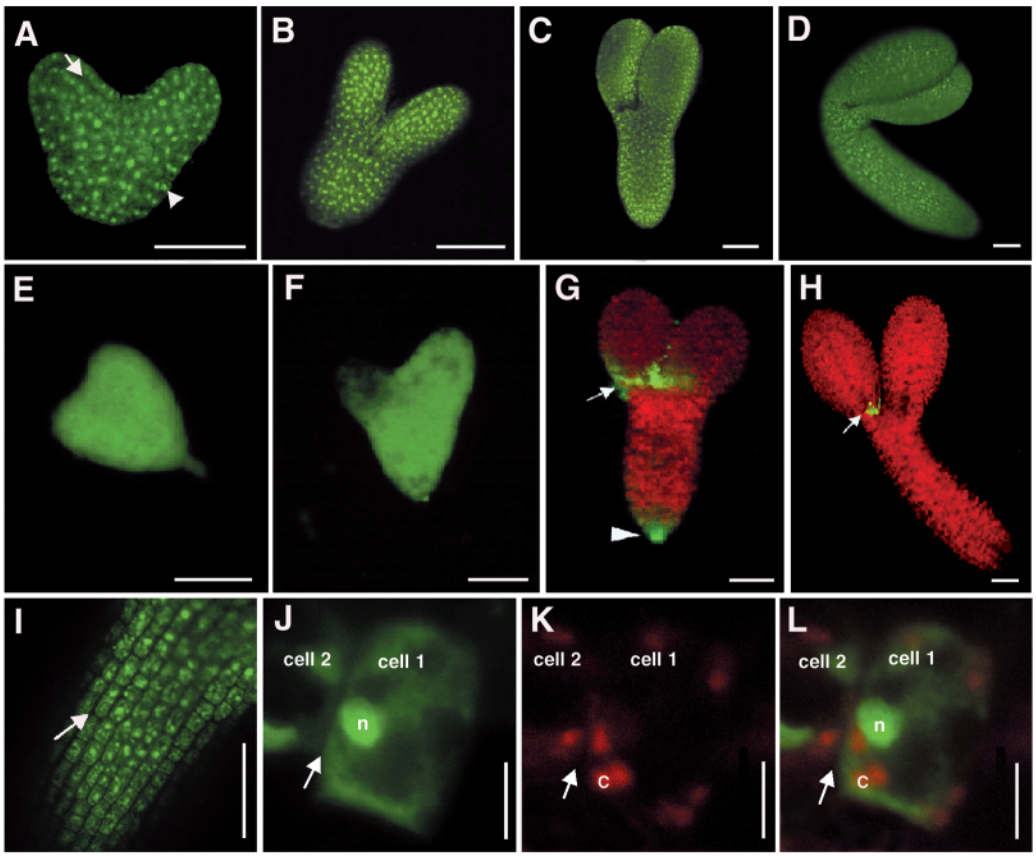

Fig. 3. Characterization of cell-to-cell transport in *Arabidopsis* wild-type embryos. L*er* embryos at different stages of development are loaded with either HPTS (A-D, I-L) or 10 kDa F-dextran (E-H). All cells in embryos allow the movement of HPTS, indicating that the embryo constitutes a single symplastic domain, from early heart (A), late heart (B), early torpedo (C), to mid-torpedo (D) stages of embryo development. Cellular localization of HPTS shows the tracer in the cytoplasm as well as the nuclei (arrowhead in A) but excluded from apoplastic regions (arrow in A). (I) Higher magnification of part of the root of the embryo in D showing HPTS distribution. (J-L) Detail of two single cells from I. Chlorophyll autofluorescence (c) marks the cytoplasm. HPTS is found both in cytoplasm, indicated by chloroplasts, and nuclei (n). L combines the images from J and K. In contrast to HPTS, 10 kDa F-dextrans move only in early heart (E) and mid heart (F) embryos. Early (G) and mid (H) torpedo embryos do not allow the movement of corresponding dextran. Instead, small numbers of cells are loaded at the tip of radicle (arrowhead) and the region where cotyledons join the hypocotyl (arrow). The images in A-D and I-L are optical sections captured by confocal laser scanning microscopy. Images in E-H were obtained by epifluorescence microscopy, and are therefore less highly resolved (see Materials and Methods for detail). Scale bars, 50 μm in A-I; 5 μm in J-L.

localization of 10 kDa F-dextran is limited to the cells at the broken edge. Fig. 4C shows similar results of F-dextran uptake to single protodermal cells; the adjacent protodermal cells are devoid of tracer, either because they are intact (failure of probe uptake) or severely damaged (failure of probe retainment). Fig. 4D diagrams how a partially broken cell wall and plasma membrane may provide the initial entrance site for uptake (green arrow) of symplastic tracers (green circles), 10 kDa F-dextran or HPTS. Further symplastic transport (yellow arrows) is then determined by the SEL of plasmodesmata connected to cells at the partially broken edge.

Data revealing the *direction* of tracer movement further support that probe uptake occurs initially from broken cells at the edges of damaged regions. This conclusion derives from time course studies. Mid-torpedo embryos were incubated with HPTS for shorter times (1-3 minutes) (Fig. 5). A small number of cells at the base of the detached cotyledons are initially loaded with HPTS (Fig. 5A). Instead of even progress toward the top, HPTS first moves to the center (Fig. 5B) and then distributes radially into surrounding ground tissues and protodermal layers, eventually transporting throughout the cotyledon (Fig. 5C,D). In whole embryos, HPTS moves into the radicle and then throughout the hypocotyl (Fig. 5E,F). Probe loading and immediate washing results in a 'pulse' of tracer. For example, as the probe moves up the hypocotyl the tip of the radicle shows only weak fluorescence. Both "ends" delimiting the region of high fluorescence in the hypocotyl then indicate the site of initial loading (radicle) and site of continued transport, at the base of the cotyledons (asterisked). (See also Fig. 6F below, for *ise1* loading with dextran.)

Symplastic tracer movement within mutant embryos

Studies with wild-type embryos revealed a window of time, corresponding to the mid-torpedo stage, when symplastic transport of large 10 kDa F-dextrans ceased. Thus, we used this developmental time to screen for embryo-defective lines with the ability to continue to traffic dextrans. In contrast to wild-type mid-torpedo embryos, *ise1* homozygous mutant embryos maintain a large SEL (Table 1). 89.2% of *ise1* embryos (66/74) allowed symplastic probe movement through most of the

Table 1. Comparison of movement frequency of 10 kDa F-dextran in wild-type and *ise1* mutant embryos of *Arabidopsis*

	Heart embryos	Early torpedo embryos	Mid torpedo embryos
L*er* WT	50% (9*/18†)	19.4% (7/36)	0% (0/58)
ise1/ ise1	ND	ND	89.2% (66/74)

L*er* WT: Landsberg *erecta* wild type.
*Number of embryos allowing the movement of tracers. Probes are considered to move between cells of embryos when more than half of the cells in embryos exhibit green fluorescence.
†Number of embryos tested.

embryo, when sibling wild-type embryos did not (0/58). *ise1* embryos typically allowed the cell-to-cell movement of 10 kDa F-dextrans throughout the entire hypocotyl and the radicle (Fig. 6F). In many *ise1* embryos, 10 kDa F-dextran also moved cell-to-cell into the bases of the cotyledons. 10 kDa F-dextrans were located consistently in cytoplasmic regions as well as nuclei (Fig. 6G, arrowhead). Unloaded apoplastic regions appeared as dark lines (Fig. 6G, arrow), demarcating the loaded cytoplasm of individual cells.

Smaller symplastic tracers, such as HPTS (524 Da) and Cascade Blue (596 Da, not shown), were also loaded into *ise1* mutant embryos to examine whether *ise1* embryos consist of a single symplastic domain. As in wild-type embryos, HPTS moved throughout all cells of *ise1* embryos (Fig. 6H). *ise1*

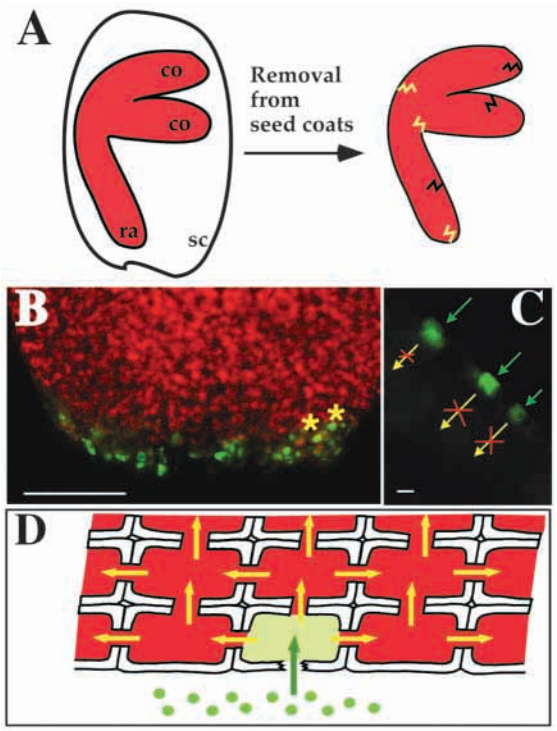

Fig. 4. Uptake and subsequent movement of symplastic tracers in cells of wild-type mid-torpedo embryos. (A) When embryos are removed from their seed coats, physical damage occurs in a subset of cells. As a result, small regions of cell walls and plasma membranes are broken to a sub-lethal level to provide an initial entrance site for uptake of symplastic tracers such as HPTS and F-dextran, which do not usually cross plasma membranes. Yellow jagged lines indicate the most common site of damage in our loading assay (see Results). Black jagged lines the random abraded sites on the protodermal layer, which are observed less frequently. co, cotyledon; ra, radicle; sc, seed coat. (B) A small number of cells at the base of the detached cotyledons from mid-torpedo embryos are cytoplasmically loaded with 10 kDa F-dextran (asterisks). Yet further movement to neighboring cells does not occur so that rest of the cells show only chlorophyll auto-fluorescence (red). Scale bar, 50 μm. (C) A typical example of loaded cells in a region at the edge of the protodermal layer where abrasion has occurred (marked as black jagged lines in A). Individual cells in the protodermal layer take up 10 kDa F-dextrans (green arrows) and show cytoplasmic localization of the probe. However, subsequent movement of the probe is inhibited (yellow arrows with red X). Scale bar, 5 μm. (D) A diagram showing that a partially broken cell wall and plasma membrane (jagged edge) may provide the initial entrance site for uptake (green arrow) of symplastic tracers, F-dextran or HPTS (green circles). Further symplastic transport (yellow arrows) is then determined by the SEL of plasmodesmata and the size of symplastic tracers introduced.

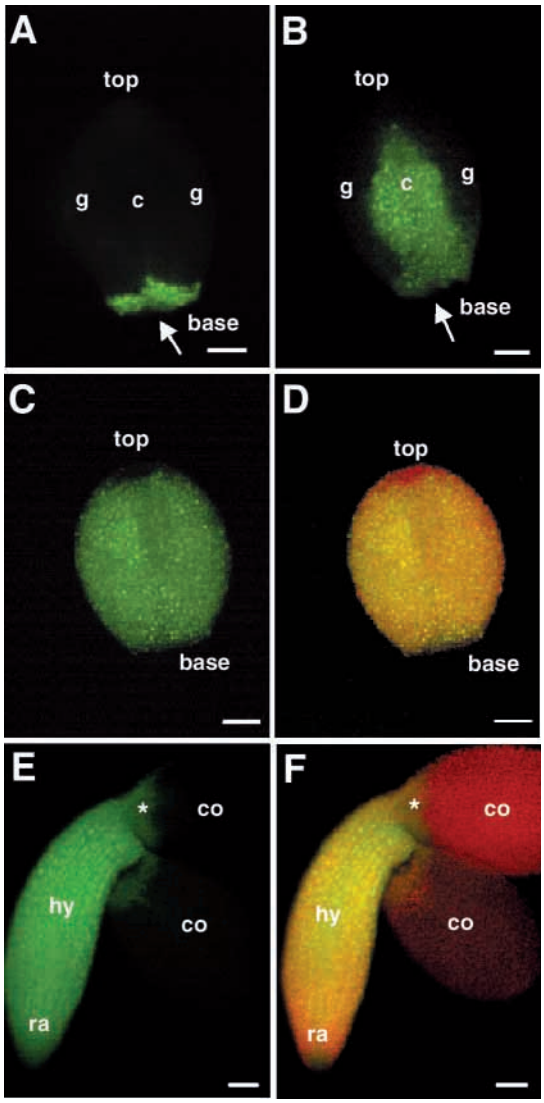

Fig. 5. Tracer loading and movement in wild-type embryos. Mid-torpedo embryos were incubated with HPTS for a shorter amount of time (1-3 minutes versus 5 minutes in other experiments) to allow observation of partially loaded embryos. (A) A detached cotyledon reveals the movement of HPTS only in a small number of cells at the base. Arrow indicates the direction of probe movement. (B) A detached cotyledon partially loaded in the center (c), and the tracer has subsequently spread into ground tissues (g). (C) A detached cotyledon showing complete loading with HPTS. (D) The same cotyledon as in C viewed with a different filter set allowing visualization of combined chlorophyll and FITC fluorescence. Loaded region with HPTS appears yellowish green owing to the additive effect between red autofluorescence from chlorophyll and green emission from HPTS. (E) A whole embryo, fully loaded with HPTS in its radicle (ra) and hypocotyl (hy), but partially loaded at the base (*) of cotyledons (co). (F) The same embryo as in E monitored with a different filter set allowing visualization of combined chlorophyll and FITC fluorescence. Images were obtained by using Chroma FITC (HPTS fluorescence; A,B,C,E) and Zeiss FITC (chlorophyll plus HPTS fluorescence; D,F) filter sets on a compound epifluorescence microscope (see Materials and Methods). Scale bars, 50 μm.

embryos showed well arranged cell files particularly in the hypocotyl and the radicle (Fig. 6F,H). The overall shape of the embryo was not markedly different from wild type, although the cotyledons were typically smaller. *ise1* embryos do not have severe morphological defects common in known cell wall and cytokinesis mutants, such as *keule*, *knolle* and *cyt1* (Assaad et al., 2001; Lauber et al., 1997; Nickle and Meinke, 1998). In these mutants, cells are often grossly enlarged and irregularly shaped, and planes of cell divisions are variably mis-oriented. Consequently, the overall shape of the embryo is markedly different from wild type. Enlarged multinucleated cells with incomplete cell walls are clearly visible following loading with HPTS (Fig. 6E). *ise2* (*emb25*) mutant embryos display a similar overall morphology compared to *ise1*, and allowed similar symplastic movement of the 10 kDa F-dextrans throughout the radicle and hypocotyl (not shown).

In summary, the time when morphological defects of *ise* mutants are manifested, corresponds to the time when wild-type embryos discontinue cell-to-cell traffic of 10 kDa dextran. That *ise* mutants continue to traffic 10 kDa dextrans suggests that this transport phenotype is correlated with their developmental retardation, and that *ise* mutants are altered in

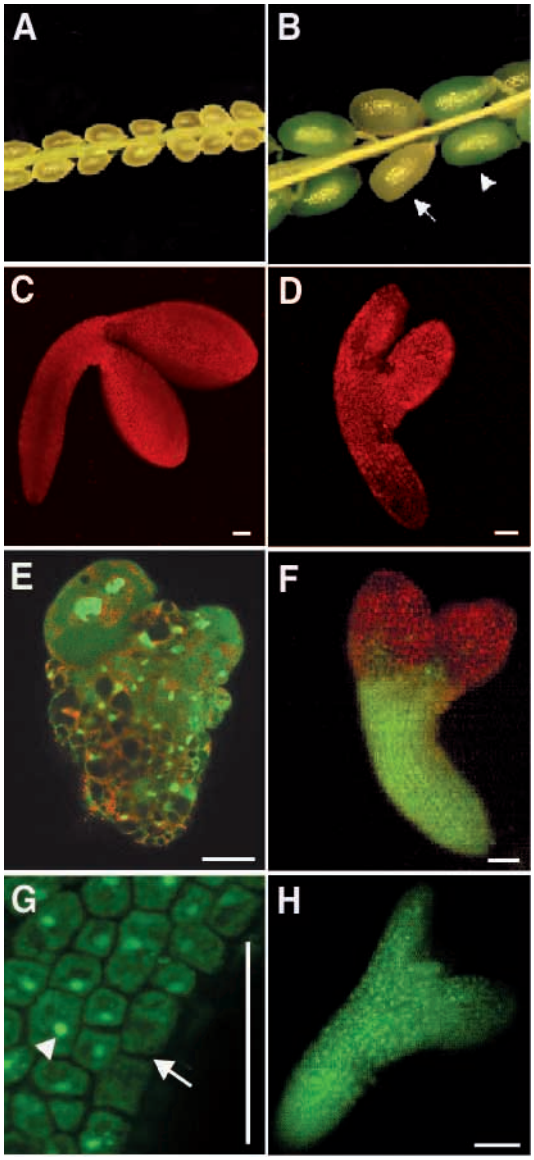

Fig. 6. Cell-to-cell movement of fluorescent tracers in *ise1* mutant embryos of *Arabidopsis*. (A) Immature siliques of both wild-type and +/*ise1* heterozygous plants contain seeds developing synchronously during early embryo development, up to the heart stage. (B) A later stage silique of +/*ise1* heterozygous plants contains dark green seeds (arrowhead) and light green seeds (arrow) in a ratio of 3:1. Seeds are 0.5 mm in length. (C,D) Embryos from the same silique; dark green seeds contain mid-torpedo wild-type embryos (C) and light green seeds contain *ise1*/*ise1* mutant embryos (D), both showing red chlorophyll autofluorescence. (E) A *keule* embryo at torpedo stage loaded with HPTS. (F) A *ise1*/*ise1* embryo allow the movement of 10 kDa F-dextran. The hypocotyl and the radicle show uniform and complete loading, and the cotyledons show partial loading at their bases. (G) Detail of the hypocotyl in F. 10 kDa F-dextran localizes in the cytoplasm as well as nuclei (arrowhead), but not in the cell wall in apoplastic regions (arrow). (H) A *ise1*/*ise1* embryo fully loaded with HTPS, showing that the *ise1* embryo constitutes a single symplast with open plasmodesmata. Scale bars, 50 μm.

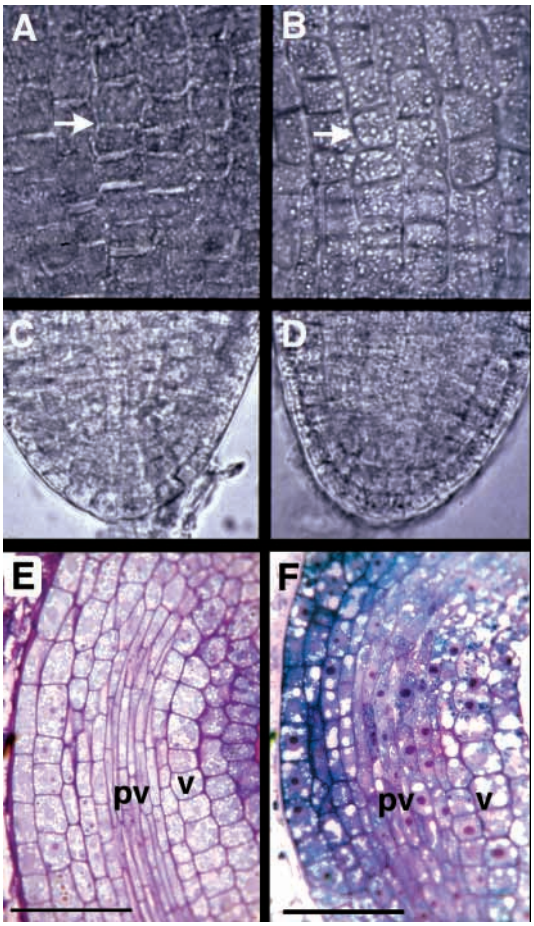

Fig. 7. Light micrographs of mid-torpedo embryos. At the mid-torpedo stage, wild-type (A,C) and sibling *ise1* mutant (B,D) embryos are similar in cell size and regular patterns of cell division (arrows) both in the hypocotyl (A,B) and the radicle (C,D) viewed with Nomarski optics. Toluidine Blue staining of hypocotyl thin sections of wild-type (E) and mutant (F) embryos shows that cells in the provascular regions (pv) are narrow and elongated in both. Vacuoles (v) in mutant cells (F) are larger in size and fewer in number than in cells of wild-type (E). Scale bars, 40 μm.

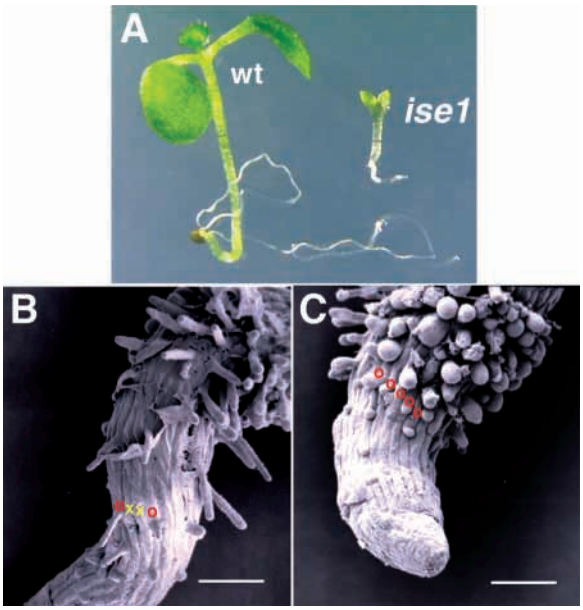

Fig. 8. Postgermination phenotype of *ise1* mutant. (A) Wild-type (wt) and sibling *ise1* seedlings 18 days postgermination on culture plates. At this stage the wild-type seedling has 4 true leaves with trichomes as well as an elongated primary root, but the mutant has only a pair of macroscopic cotyledons and a very short primary root. (B) Scanning electron micrograph of the root epidermis of wild-type 2 days postgermination shows cell files with root hairs (red circles) and without root hairs (yellow X). In the *ise1* root epidermis (C), however, all cell files produce root hairs (red circles) indicating a homogenization of cell fate. Scale bars, 50 μm.

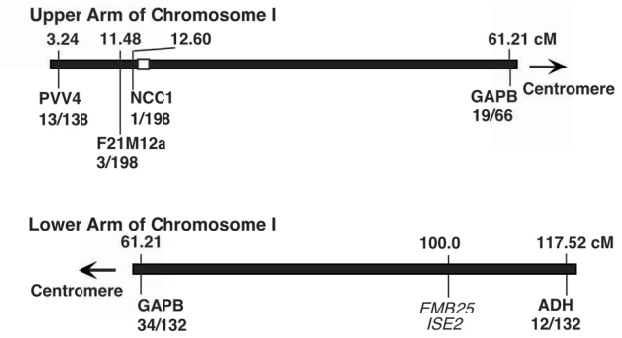

Fig. 9. The molecular genetic map of *ISE* genes on chromosome I. *ISE1* gene maps between CAPS markers, NCC1 and GAPB on chromosome I. The black bar represents chromosome I and numbers above the bar indicate the genetic location of corresponding markers shown below. *ISE1* maps 0.51 cM apart from NCC1 and its approximate location is marked as a white block on the bar. *ISE2* maps between GAPB and ADH on chromosome I and its approximate location is marked as a vertical line. The genetic map positions given are taken from the Lister and Dean recombinant inbred (RI) map from The *Arabidopsis* Information Resource (TAIR, http://www.*Arabidopsis*.org/search/marker_search.html) as well as Nottingham *Arabidopsis* Stock Centre (NASC) RI map (http://nasc.nott.ac.uk/new_ri_map.html). The number of recombinants and the total number of chromosomes tested are noted with a slash under the corresponding markers.

plasmodesmata function. Close to 5000 lines examined that had embryo defects evident during the torpedo stage of embryogenesis, did not traffic 10 kDa F-dextrans. Thus, the *ise* phenotype is specific to few lines, and is not a general defect simply associated with altered developmental patterning.

Morphological characterization of *ise1*

Homozygous *ise1* seeds resemble wild-type seeds during early stages of development; Fig. 6A shows seeds containing heart stage embryos and the mutant seeds cannot be distinguished. Wild-type seeds (both +/+ and +/*ise1*) enlarge and turn darker green during the torpedo stage of embryo development due to chlorophyll accumulation in embryos, visible through the translucent seed coats. *ise1* mutant seeds, however, are retarded in morphogenesis and remain light green in color compared to their dark green wild-type siblings at this stage (Fig. 6B). Both mutant and wild-type seeds turn brown at maturity. No unfertilized ovules were observed in siliques from *ise1* heterozygotes segregating for wild-type and mutant embryos (not shown), indicating that *ISE1* gene acts postfertilization.

ise1 mutant embryos are distinguished morphologically from wild-type siblings at the mid-torpedo stage. When wild-type embryos are in the mid-torpedo stage, *ise1* mutants first appear as more heart-shaped corresponding in size to a wild-type early torpedo (not shown). When wild-type embryos are at the mid-torpedo stage, *ise1* embryos continue to grow and appear like early torpedo embryos in size and morphology (compare Fig. 6C and 6D). At this time, *ise1* embryos are approximately 50% smaller in size than wild type; growth subsequent to this time is slow. At maturity, *ise1* embryos appear mid-torpedo in shape and size.

Nomarski views in Fig. 7A-D show that the organization of cell files in the hypocotyl and radicle regions of wild-type and *ise1* mutant embryos are comparable. Fig. 7E and F shows thin sections from hypocotyl regions of wild-type and *ise1* mutant embryos stained with Toluidine Blue. The provascular tissues (pv) are well formed in mutant embryos, as in wild type. The only notable difference is that cells in mutant tissues have a smaller number of large vacuoles (v), whereas cells in wild-type embryos contain a large number of small vacuoles. Taken together, the planes of cell division as well as overall tissue differentiation appear unaffected in *ise1*.

ise1 seeds are tolerant to desiccation, and germinate on agar culture medium to produce very small and stunted plants (Fig. 8A). A further hint that plasmodesmata regulation is altered in *ise1* is provided by scanning electron micrographs comparing wild-type and *ise1* primary roots postgermination (Fig. 8B,C). While wild-type root epidermal cell files alternate in production of root hairs (Benfey and Scheres, 2000), all epidermal cell files in *ise1* roots produces root hairs. These data suggest that alteration of symplastic pathways may lead to homogenization of cell types (see Discussion).

Genetics and molecular mapping of the *ISE* genes

The *ise1* mutant phenotype segregates as a single recessive trait. In wild-type plants, the average length of siliques is 12.5±0.3 mm (n=20) and each silique contains 60±2 seeds. *ise1* heterozygous plants (+/*ise1*) have siliques with average length of 12.3±0.3 mm (n=20) and individual siliques contain 59±2 seeds displaying 3:1 segregation of normal to homozygous mutant seeds (880:300, χ^2=0.08, P>0.5). When *ise1* heterozygous plants (+/*ise1*) are crossed to wild-type plants, 1:1 segregation ratios of wild-type to heterozygotes (34:36, χ^2=0.06,

P>0.5) are observed in F_1 progeny; heterozygosity is determined by examination of siliques for the segregation of mutant embryos in F_2 progeny from selfed F_1 plants. The overall segregation of heterozygotes to wild-type plants in F_2 progenies is 2:1 (937:1880, χ^2=0.06, *P*>0.5), consistent with the inheritance of a single recessive locus and seedling lethal phenotype.

Heterozygous +/*ise* plants in L*er* were crossed to wild-type female plants of the Col ecotype to test the linkage of *ISE* loci with previously mapped polymorphic markers (Chang et al., 1988). Heterozygous F_1 plants were selfed to produce progeny segregating chromosomes from both parents. Molecular mapping was performed using DNA from F_2 wild-type plants which are homozygous for the Col allele at the *ISE* loci (Col/Col), as homozygous mutants plants (L*er*/L*er*) are seedling lethal. Wild-type individuals were selected by checking that their immature siliques contained only wild-type embryos. PCR-based biallelic markers, CAPS and SSLPs, were used to map the *ISE1* locus to the 13 cM region of chromosome I (Fig. 9). Using the same method, *ISE2* was mapped to 100 cM on chromosome I. This location is close to a known embryo-defective line, *emb25* (Franzmann et al., 1989). A genetic complementation test indicated that *ise2* was allelic to *emb25*.

DISCUSSION

Plants may be viewed as a mosaic of symplastic domains that share a common cytoplasm bounded by the plasma membranes of connected cells, that may act as relatively distinct operational subunits (Ehlers et al., 1999; Erwee and Goodwin, 1985). The formation of symplastic domains often precedes the appearance of morphologically distinct structures in development (Gisel et al., 1999; Palevitz and Hepler, 1985). To date, cell-to-cell trafficking patterns during plant embryogenesis have not been extensively studied. The relatively simple fluorescent tracer loading method developed here allows embryos of *Arabidopsis* to be easily assessed for symplastic transport via plasmodesmata. All cells of the embryo from early heart to mid-torpedo stages traffic small probes between 0.5 and 3 kDa. Surprisingly, even large dextrans of 10 kDa traffic throughout the embryo until the early torpedo stage. However, while small probes continue to traffic, there is a developmental transition that begins between heart and early torpedo stages, when 10 kDa tracers are no longer able to traffic throughout the embryo. Thus, in wild-type embryos plasmodesmata are open in all cells throughout all stages, as monitored by small tracers; however, the degree of dilation changes, as monitored by 10 kDa dextrans. Interestingly, the embryo remains a single symplast until at least the mid-torpedo stage studied here, as whenever tracer (small or large) traffics, it does so throughout the entire embryo. Future studies will begin to address small and large tracer transport in post-torpedo embryos and early seedlings.

The down-regulation of plasmodesmata aperture correlates with the initiation of autotrophic development in embryos. Early *Arabidopsis* embryos depend upon the suspensor connection to the maternal endosperm tissues for nutrients and growth regulators. The suspensor connection degenerates by the early torpedo stage. Embryos start synthesizing chlorophyll and become green at the early heart stage (Meinke and Sussex, 1979). The granal system in chloroplasts, essential for photosynthesis and autotrophic growth, is well developed by the torpedo stage of embryo development (Mansfield and Briarty, 1991). Embryogenesis up to this point has been recently referred to as the growth phase (Raz et al., 2001). Thus, the decrease in SEL of plasmodesmata corresponds to when embryos have determined most of their basic essential tissues and organ types, and subsequent growth is largely due to expansion. Down-regulation of plasmodesmata may aid the onset of developmental programming towards dormancy at seed maturation.

The down-regulation of plasmodesmata coupled to developmental progression has been documented in other tissues. Symplastic transport within the shoot apical meristem is temporarily restricted during the transition to floral development (Gisel et al., 1999). Also in tobacco leaves during the transition from sink (the less mature, net carbon importing) to source (the more mature, net carbon exporting) tissue, plasmodesmata are substantially down-regulated with a structural switch from simple to branched forms (Crawford and Zambryski, 2001; Oparka et al., 1999). GFP (27 kDa) and GFP-fusion proteins greater than 50 kDa can freely move in sink leaves. In contrast, such GFP tracers move to a lesser extent in source leaves. In embryo sacs of *Torenia fournieri* (Han et al., 2000), the SEL of plasmodesmata between the central cell and the egg apparatus cells decreases progressively from 10 kDa to 3 kDa, as the embryo sac matures.

Arabidopsis root epidermal cells are symplastically coupled in the undifferentiated cells of the root meristematic region and the elongation zone. These epidermal cells, however, become symplastically isolated as they mature and differentiate (Duckett et al., 1994). Interestingly, *ise1* mutants exhibit morphological defects in the roots of germinating mutant seedlings. All *ise1* root epidermal cell files produce root hairs, whereas in the wild-type, root hair producing cell files alternate with cell files that do not produce root hairs (Benfey and Scheres, 2000). The homogenization of cell types in the root epidermis of *ise1* may be due to the lack of symplastic isolation that normally occurs in wild-type *Arabidopsis* root epidermal cells.

Dye coupling in the embryo sac of *Torenia fournieri* using microinjection was studied, as its embryo sac is relatively large, and protrudes from the ovule (Han et al., 2000). In contrast, *Arabidopsis* embryos are very small and enclosed by maternal tissues, making it difficult to apply methods such as microinjection or particle bombardment. Further, such methods can lead to plasmodesmata closure if performed at high pressures (Itaya et al., 1997; Itaya et al., 2000). Here, extrusion of embryos from their seed coats was found to result in sub-lethal cell damage at the radicle tips and at cotyledon-hypocotyl junctions; such damaged cells provide sites of entry for hydrophilic fluorescent symplastic tracers. Tracers were taken up from liquid medium bathing the embryos, via endogenous pathways, without any application of pressure. In a similar method called scrape-loading used for mammalian cells, a tear in the plasma membrane of cells creates an initial entrance point for symplastic tracers into the cytoplasm without affecting cell viability (Blomstrand et al., 1999; el-Fouly et al., 1987; Saleh and Takemoto, 2000). This method is widely used to monitor animal cell-to-cell communication via gap junctions (Carruba et al., 1999). Another similar method

is a commonly used tool in virus inoculation to plant leaves, called 'mechanical transmission'. For instance, tobacco mosaic virus moves its nucleic acids through plasmodesmata during infection. Yet its initial entrance to plant cells occurs through transient breaks in the plasma membrane caused by mechanical abrasion (Walkey, 1985).

ise1 and *ise2* mutant embryos have an increased size exclusion limit of plasmodesmata

The present studies were undertaken to gain insight into cell-to-cell trafficking patterns during embryogenesis, a critical stage in plant development. In addition, these studies were provoked by the need to identify genes involved in plasmodesmata structure and function. It was reasoned that mutations in such genes would lead to gross alterations in plant development and loss of viability; such mutants would likely be detected as defective embryos. The non-invasive tracer loading method developed here was applied to screen embryo-defective lines for altered patterns of tracer movement. Our analysis with wild-type embryos uncovered a window of time when plasmodesmata down-regulate their ability to traffic 10 kDa F-dextrans. Thus, we screened embryo-defective mutants at the torpedo stage for the ability to continue to traffic 10 kDa F-dextrans at a time when wild-type embryos cannot. Fourteen lines, out of 5000 examined, were designated *increased size exclusion limit* (*ise*), as they allowed trafficking at the mid-torpedo stage of development. Only a small portion of lines (0.28%) with defects at this stage, displayed altered tracer movement. Thus, the *ise* phenotype is not generally associated with altered development at the torpedo stage. One line, *ise1*, characterized in detail herein, continued to allow 10 kDa F-dextran movement even at late torpedo stage (I. K., unpublished results).

There are 4 general classes of mutations that might be expected to lead to larger SEL, (1) those affecting cytokinesis, cell plate, or cell wall structure, (2) mutations in plasmodesmata structural genes, (3) mutations in genes that directly regulate plasmodesmatal function, or (4) mutations in genes that indirectly affect plasmodesmata aperture. The most logical way to distinguish these possibilities might be to perform detailed ultrastructural studies of cell wall regions containing plasmodesmata in mutants. However, recent data suggest this approach is not adequate. A maize mutant, *sxd1*, shows clear modification in ultrastructure of plasmodesmata (Russin et al., 1996); however, molecular cloning reveals the *SXD1* gene encodes a nuclear encoded chloroplast localized protein (Provencher et al., 2001). Thus, knowing the *SXD1* gene does not explain how its mutation leads to alterations of plasmodesmata ultrastructure. In turn, these data provoke the prediction that critical players in plasmodesmata function or regulation may not induce a readily observable alteration in plasmodesmata architecture. In fact, preliminary electron microscopic studies suggest that plasmodesmata in *ise1* are not dramatically altered (data not shown).

With regard to *ise1* embryos, the increased SEL phenotype is not likely to be caused by defects in either the plasma membrane or the cell wall as *ise1* embryos showed well arranged cell files, and the overall morphology of *ise1* embryos resembled wild type. Mutant embryos with gapped or incomplete cell walls, such as *knolle* (Lukowitz et al., 1996), *keule* (Assaad et al., 1996; Assaad et al., 2001) and *cyt1* (Nickle and Meinke, 1998) have severe overall morphological defects and can be easily identified. HPTS was present only in cytoplasmic regions of the *ise* mutants and was not observed in cell wall perimeters, implying tracer trafficked cell-to-cell via narrow plasmodesmata bridges that span the cell wall between adjacent cells. As gross morphology of cells, tissues, and plasmodesmata is preserved in *ise* mutants, the mutations probably do not affect a major plasmodesmata structural component. Thus, *ise* mutations may affect a minor plasmodesmata structural component, or more likely affect genes that regulate plasmodesmata function (directly or indirectly). Molecular studies to clone *ISE* genes are underway. The determination of their encoded products will provide insight into how these dynamic plasmodesmata channels function during embryonic development.

We thank Steve Ruzin and Denise Schichnes of the Center for Biological Imaging for invaluable advice on microscopy. This work was supported by NIH grant GM45244 and by a NSF postdoctoral fellowship to F. D. H.

REFERENCES

Assaad, F. F., Huet, Y., Mayer, U. and Juergens, G. (2001). The cytokinesis gene KEULE encodes a Sec1 protein that binds the syntaxin KNOLLE. *J. Cell Biol.* **152**, 531-543.

Assaad, F. F., Mayer, U., Wanner, G. and Juergens, G. (1996). The KEULE gene is involved in cytokinesis in Arabidopsis. *Mol. Gen. Genet.* **253**, 267-277.

Baulcombe, D. (2001). RNA silencing. Diced defence. *Nature* **409**, 295-296.

Benfey, P. N. and Scheres, B. (2000). Root development. *Curr. Biol.* **10**, R813-815.

Blomstrand, F., Aberg, N. D., Eriksson, P. S., Hansson, E. and Ronnback, L. (1999). Extent of intercellular calcium wave propagation is related to gap junction permeability and level of connexin-43 expression in astrocytes in primary cultures from four brain regions. *Neuroscience* **92**, 255-265.

Botha, C. E. J. and Cross, R. H. M. (2000). Towards reconciliation of structure with function in plasmodesmata: Who is the gatekeeper? *Micron* **31**, 713-721.

Carrington, J. C., Kasschau, K. D., Mahajan, S. K. and Schaad, M. C. (1996). Cell-to-cell and long-distance transport of viruses in plants. *Plant Cell* **8**, 1669-1681.

Carruba, G., Webber, M. M., Bello-Deocampo, D., Amodio, R., Notarbartolo, M., Deocampo, N. D., Trosko, J. E. and Castagnetta, L. A. (1999). Laser scanning analysis of cell-cell communication in cultured human prostate tumor cells. *Anal. Quant. Cytol. Histol.* **21**, 54-58.

Chang, C., Bowman, J. L., Dejohn, A. W., Lander, E. S. and Meyerowitz, E. M. (1988). Restriction fragment length polymorphism linkage map for *Arabidopsis thaliana*. *Proc. Natl. Acad. Sci. USA* **85**, 6856-6860.

Chisholm, S. T., Mahajan, S. K., Whitham, S. A., Yamamoto, M. L. and Carrington, J. C. (2000). Cloning of the Arabidopsis RTM1 gene, which controls restriction of long-distance movement of tobacco etch virus. *Proc. Natl. Acad. Sci. USA* **97**, 489-494.

Crawford, K. M. and Zambryski, P. (2000). Subcellular localization determines the availability of non-targeted proteins to plasmodesmatal transport. *Curr. Biol.* **10**, 1032-1040.

Crawford, K. M. and Zambryski, P. C. (2001). Non-targeted and targeted protein movement through plasmodesmata in leaves in different developmental and physiological states. *Plant Physiol.* **125**, 1802-1812.

Ding, B. (1998). Intercellular protein trafficking through plasmodesmata. *Plant Mol. Biol.* **38**, 279-310.

Ding, B., Turgen, R. and Parthasarathy, M. V. (1992). Substructure of freeze-substituted plasmodesmata. *Protoplasma* **169**, 28-41.

Duckett, C. M., Oparka, K. J., Prior, D. A. M., Dolan, L. and Roberts, K. (1994). Dye-coupling in the root epidermis of *Arabidopsis* is progressively reduced during development. *Development* **120**, 3247-3255.

Ehlers, K., Binding, H. and Kollmann, R. (1999). The formation of symplasmic domains by plugging of plasmodesmata: A general event in plant morphogenesis? *Protoplasma* **209**, 181-192.

el-Fouly, M. H., Trosko, J. E. and Chang, C. C. (1987). Scrape-loading and dye transfer. A rapid and simple technique to study gap junctional intercellular communication. *Exp. Cell Res.* **168**, 422-430.

Erwee, M. G. and Goodwin, P. B. (1985). Symplast domains in extrastelar tissues of *Egeria densa*. *Planta* **163**, 9-19.

Franzmann, L., Patton, D. A. and Meinke, D. W. (1989). In vitro morphogenesis of arrested embryos from lethal mutants of Arabidopsis thaliana. *Theor. Appl. Genet.* **77**, 609-616.

Franzmann, L. H., Yoon, E. S. and Meinke, D. W. (1995). Saturating the genetic map of Arabidopsis thaliana with embryonic mutations. *Plant J.* **7**, 341-350.

Gisel, A., Barella, S., Hempel, F. D. and Zambryski, P. C. (1999). Temporal and spatial regulation of symplastic trafficking during development in *Arabidopsis thaliana* apices. *Development* **126**, 1879-1889.

Glazebrook, J., Drenkard, E., Preuss, D. and Ausubel, F. M. (1998). Use of cleaved amplified polymorphic sequences (CAPS) as genetic markers in Arabidopsis thaliana. In *Arabidopsis Protocols*, vol. 82 (ed. J. M. Martinez-Zapater and J. Salinas), pp. 173-182. Totowa: Human Press Inc.

Goldberg, R. B., De Paiva, G. and Yadegari, R. (1994). Plant embryogenesis: Zygote to seed. *Science* **266**, 605-614.

Goodwin, P. B. (1983). Molecular size limit for movement in the symplast of the *Elodea* leaf. *Planta* **157**, 124-130.

Gunning, B. E. S. (1976). Introduction to plasmodesmata. In *Intercellular Communication in Plants: Studies on Plasmodesmata*, (ed. B. E. S. Gunning and R. W. Robards), pp. 1-12. New York: Springer-Verlag.

Han, Y. Z., Huang, B. Q., Zee, S. Y. and Yuan, M. (2000). Symplastic communication between the central cell and the egg apparatus cells in the embryo sac of *Torenia fournieri* Lind. before and during fertilization. *Planta* **211**, 158-162.

Hantke, S. S., Carpenter, R. and Coen, E. S. (1995). Expression of floricaula in single layers of periclinal chimeras activates downstream homeotic genes in all layers of floral meristems. *Development* **121**, 27-35.

Imlau, A., Truernit, E. and Sauer, N. (1999). Cell-to-cell and long-distance trafficking of the green fluorescent protein in the phloem and symplastic unloading of the protein into sink tissues. *Plant Cell* **11**, 309-322.

Itaya, A., Hickman, H., Bao, Y., Nelson, R. and Ding, B. (1997). Cell-to-cell trafficking of cucumber mosaic virus movement protein:green fluorescent protein fusion produced by biolistic gene bombardment in tobacco. *Plant J.* **12**, 1223-1230.

Itaya, A., Liang, G., Woo, Y.-M., Nelson, R. S. and Ding, B. (2000). Nonspecific intercellular protein trafficking probed by green-fluorescent protein in plants. *Protoplasma* **213**, 165-175.

Jackson, D. (2000). Opening up the communication channels: Recent insights into plasmodesmal function. *Curr. Opin. Plant Biol.* **3**, 394-399.

Kempers, R., Prior, D. A. M., van Bel, A. J. E. and Oparka, K. J. (1993). Plasmodesmata between sieve element and companion cell of extrafascicular stem phloem of *Cucrubita maxima* permit passage of 3 kDa fluorescent probes. *Plant J.* **4**, 567-575.

Kempers, R. and Van Bel, A. J. E. (1997). Symplasmic connections between sieve element and companion cell in the stem phloem of *Vicia faba* L. have a molecular exclusion limit of at least 10 kDa. *Planta* **201**, 195-201.

Koornneef, M., Alonso-Blanco, C. and Stam, P. (1998). Genetic analysis. In *Arabidopsis Protocols*, vol. 82 (ed. J. M. Martinex-Zapater and J. Salinas), pp. 105-117. Totowa: Humana Press Inc.

Koornneef, M. and Stam, P. (1992). Genetic analysis. In *Methods in Arabidopsis Research* (ed. C. Koncz N. H. Chua and J. Schell), pp. 83-99. Cologne: World Scientific Publishing Co.

Lartey, R. T., Ghoshroy, S. and Citovsky, V. (1998). Identification of an Arabidopsis thaliana mutation (vsm1) that restricts systemic movement of tobamoviruses. *Mol. Plant-Microbe Interact.* **11**, 706-709.

Lauber, M. H., Waizenegger, I., Steinmann, T., Schwarz, H., Mayer, U., Hwang, I., Lukowitz, W. and Juergens, G. (1997). The Arabidopsis KNOLLE protein is a cytokinesis-specific syntaxin. *J. Cell Biol.* **139**, 1485-1493.

Lazarowitz, S. G. and Beachy, R. N. (1999). Viral movement proteins as probes for intracellular and intercellular trafficking in plants. *Plant Cell* **11**, 535-548.

Lucas, W. J., Bouche-Pillon, S., Jackson, D. P., Nguyen, L., Baker, L., Ding, B. and Hake, S. (1995). Selective trafficking of KNOTTED1 homeodomain protein and its mRNA through plasmodesmata. *Science* **270**, 1980-1983.

Lukowitz, W., Mayer, U. and Juergens, G. (1996). Cytokinesis in the Arabidopsis embryo involves the syntaxin-related KNOLLE gene product. *Cell* **84**, 61-71.

Mansfield, S. G. and Briarty, L. G. (1991). Early embryogenesis in *Arabidopsis thaliana*: II. The developing embryo. *Can. J. Bot.* **69**, 461-476.

Mayer, U., Ruiz, R. A. T., Berleth, T., Misera, S. and Juergens, G. (1991). Mutations affecting body organization in the Arabidopsis embryo. *Nature* **353**, 402-407.

Meinke, D. W. (1994). Seed developement in *Arabidopsis thaliana*. In *Arabidopsis*, vol. 27 (ed. E. M. Meyerowitz and C. R. Somerville), pp. 253-295. Plainview: Cold Spring Harbor Laboratory Press.

Meinke, D. W. and Sussex, I. M. (1979). Embryo-lethal mutants of Arabidopsis thaliana. A model system for genetic analysis of plant embryo development. *Dev. Biol.* **72**, 50-61.

Moore-Gordon, C. S., Cowan, A. K., Bertling, I., Botha, C. E. J. and Cross, R. H. M. (1998). Symplastic solute transport and avocado fruit development: A decline in cytokinin/ABA ration is related to appearance of the Hass small fruit variant. *Plant Cell Physiol.* **39**, 1027-1038.

Mourrain, P., Beclin, C., Elmayan, T., Feuerbach, F., Godon, C., Morel, J. B., Jouette, D., Lacombe, A. M., Nikic, S., Picault, N. et al. (2000). Arabidopsis SGS2 and SGS3 genes are required for posttranscriptional gene silencing and natural virus resistance. *Cell* **101**, 533-542.

Nickle, T. C. and Meinke, D. W. (1998). A cytokinesis-defective mutant of Arabidopsis (cyt1) characterized by embryonic lethality, incomplete cell walls and excessive callose accumulation. *Plant J.* **15**, 321-332.

Oparka, K. J. (1991). Uptake and compartmentation of fluorescent probes by plant cells. *J. Exp. Bot.* **42**, 565-580.

Oparka, K. J. and Prior, D. A. M. (1992). Direct evidence for pressure-generated closure of plasmodesmata. *Plant J.* **2**, 741-750.

Oparka, K. J., Roberts, A. G., Boevink, P., Santa Cruz, S., Roberts, I., Pradel, K. S., Imlau, A., Kotlizky, G., Sauer, N. and Epel, B. (1999). Simple, but not branched, plasmodesmata allow the nonspecific trafficking of proteins in developing tobacco leaves. *Cell* **97**, 743-754.

Overall, R. L., Wolfe, J. and Gunning, B. E. S. (1982). Intercellular communicationin Azolla roots. I. Ultrastructure of plasmodesmata. *Protoplasma* **111**, 134-150.

Palauqui, J.-C. and Balzergue, S. (1999). Activation of systemic acquired silencing by localised introduction of DNA. *Curr. Biol.* **9**, 59-66.

Palauqui, J.-C., Elmayan, T., Pollien, J.-M. and Vaucheret, H. (1997). Systemic acquired silencing: Transgene-specific post-transcriptional silencing is transmitted by grafting from silenced stocks to non-silenced scions. *EMBO J.* **16**, 4738-4745.

Palevitz, B. A. and Hepler, P. K. (1985). Changes in dye coupling of stomatal cells of Allium and Commelina demonstrated by microinjection of Lucifer yellow. *Planta* **164**, 473-479.

Pickard, B. G. and Beachy, R. N. (1999). Intercellular connections are developmentally controlled to help move molecules through the plant. *Cell* **98**, 5-8.

Provencher, L. M., Miao, L., Sinha, N. and Lucas, W. J. (2001). Sucrose export defective1 encodes a novel protein implicated in chloroplast-to-nucleus signaling. *Plant Cell* **13**, 1127-1141.

Raz, V., Bergervoet, J. H. and Koornneef, M. (2001). Sequential steps for developmental arrest in *Arabidopsis* seeds. *Development* **128**, 243-252.

Robards, A. W. (1971). The ultrastructure of plasmodesmata. *Protoplasma* **72**, 315-323.

Russin, W. A., Evert, R. F., Vanderveer, P. J., Sharkey, T. D. and Briggs, S. P. (1996). Modification of a specific class of plasmodesmata and loss of sucrose export ability in the sucrose export defective maize mutant. *Plant Cell* **8**, 645-658.

Saleh, S. M. and Takemoto, D. J. (2000). Overexpression of protein kinase Cgamma inhibits gap junctional intercellular communication in the lens epithelial cells. *Exp. Eye Res.* **71**, 99-102.

Schaffner, A. R. (1996). pARMS, lumtiple marker containing plasmids for easy RFLP analysis in *Arabidopsis thaliana*. *Plant Mol. Biol. Rep.* **13**, 11-16.

Sessions, A., Yanofsky, M. F. and Weigel, D. (2000). Cell-cell signaling and movement by the floral transcription factors LEAFY and APETALA1. *Science* **289**, 779-781.

Tilney, L. G., Cooke, T. J., Connelly, P. S. and Tilney, M. S. (1991). The structure of plasmodesmata as revealed by plasmolysis, detergent extraction, and protease digestion. *J. Cell Biol.* **112**, 739-747.

Tucker, E. B. (1982). Translocation in the staminal hairs of Setcreasea purpurea. I. A study of cell ultrastructure and cell-to-cell passage of molecular probes. *Protoplasma* **113**, 193-201.

Voinnet, O., Lederer, C. and Baulcombe, D. C. (2000). A viral movement protein prevents spread of the gene silencing signal in Nicotiana benthamiana. *Cell* **103**, 157-167.

Voinnet, O., Vain, P., Angell, S. and Baulcombe, D. C. (1998). Systemic spread of sequence-specific transgene RNA degradation in plants is initiated by localized introduction of ectopic promoterless DNA. *Cell* **95**, 177-187.

Waigmann, E., Lucas, W. J., Citovsky, V. and Zambryski, P. (1994). Direct functional assay for tobacco mosaic virus cell-to-cell movement protein and identification of a domain involved in increasing plasmodesmal permeability. *Proc. Nal. Acad. Sci. USA* **91**, 1433-1437.

Walkey, D. G. A. (1985). Mechanical transmission and virus isolation. In *Applied Plant Virology* (ed. D. G. A. Walkey), pp. 93-110. New York: Wiley Interscience.

West, M. A. L. and Harada, J. J. (1993). Embryogenesis in higher plants: An overview. *Plant Cell* **5**, 1361-1369.

Wolf, S., Deom, C. M., Beachy, R. N. and Lucas, W. J. (1989). Movement protein of tobacco mosaic virus modifies plasmodesmatal size exclusion limit. *Science* **246**, 377-379.

Wright, K. M. and Oparka, K. J. (1996). The fluorescent probe HPTS as a phloem-mobile, symplastic tracer: An evaluation using confocal laser scanning microscopy. *J. Exp. Bot.* **47**, 439-445.

Zambryski, P. and Crawford, K. (2000). Plasmodesmata: gatekeepers for cell-to-cell transport of developmental signals in plants. *Annu. Rev. Cell Dev. Biol.* **16**, 393-421.